Deciphering the Roles of Multicomponent Recognition Signals by the AAA+ Unfoldase ClpX

Citation: Ling, Lorraine et al. "Deciphering the Roles of Multicomponent Recognition Signals by the AAA + Unfoldase ClpX." Journal of Molecular Biology 427.18 (2015): 2966–2982.

As Published: http://dx.doi.org/10.1016/j.jmb.2015.03.008

Publisher: Elsevier

Persistent URL: http://hdl.handle.net/1721.1/107792

Version: Author's final manuscript: final author's manuscript post peer review, without publisher's formatting or copy editing

HHS Public Access

Author manuscript

J Mol Biol. Author manuscript; available in PMC 2016 September 11.

Published in final edited form as:

J Mol Biol. 2015 September 11; 427(18): 2966–2982. doi:10.1016/j.jmb.2015.03.008.

Deciphering the roles of multi-component recognition signals by the AAA+ unfoldase, ClpX

Lorraine Ling[1], **Sherwin P. Montaño**[3], **Robert T. Sauer**[1], **Phoebe A. Rice**[3], and **Tania A. Baker**[1,2,*]

[1]Department of Biology, MIT

[2]Howard Hughes Medical Institute

[3]Dept. of Biochemistry & Molecular Biology, The University of Chicago

Abstract

ATP-dependent protein remodeling and unfolding enzymes are key participants in protein metabolism in all cells. How these often-destructive enzymes specifically recognize target protein complexes is poorly understood. Here, we use the well-studied AAA+ unfoldase-substrate pair, *E. coli* ClpX and MuA transposase, to address how these powerful enzymes recognize target protein complexes. We demonstrate that the final transposition product, which is a DNA-bound tetramer of MuA, is preferentially recognized over the monomeric apo-protein through its multivalent display of ClpX recognition tags. The important peptide tags include one at the C-terminus ("C-tag") that binds the ClpX pore and a second (enhancement or "E-tag") that binds the ClpX N-terminal domain. We construct a chimeric protein to interrogate subunit-specific contributions of these tags. Efficient remodeling of MuA tetramers requires ClpX to contact a minimum of three tags (one C-tag and two or more E-tags), and that these tags are contributed by different subunits within the tetramer. The individual recognition peptides bind ClpX weakly (K_D>70μM), but when combined in the MuA tetramer, impart a high-affinity interaction (K_D~1.0 μM). When the weak C-tag signal is replaced with a stronger recognition tag, the E-tags become unnecessary and ClpX's preference for the complex over MuA monomers is eliminated. Additionally, because the spatial orientation of the tags is predicted to change during the final step of transposition, this recognition strategy suggests how AAA+ unfoldases specifically distinguish the completed "end-stage" form of a particular complex for the ideal biological outcome.

Keywords

adaptor protein; ClpXP; MuA; protein; chaperon; degron

*To whom correspondence should be addressed: phone: 617-253-3594, fax: 617-252-1852, tabaker@mit.edu.

INTRODUCTION

Cells are densely packed with proteins that have structural and/or enzymatic roles essential for life. To help respond to environmental changes, manage protein turnover, and maintain protein quality control, cells employ energy-dependent unfoldases/disaggregases and proteases of the AAA+ enzyme family[1] (ATPases associated with various cellular activities). Powered by cycles of nucleotide binding, hydrolysis, and release, these ATPases remodel complexes, solubilize aggregates, and degrade proteins when coupled with partner peptidases[1,2]. *E. coli* ClpX is arguably the best-characterized AAA+ unfoldase and is known to disassemble complexes and unfold target proteins[3,4]. ClpX can either act alone as a protein-remodeling enzyme or in a complex with the ClpP peptidase, forming the ClpXP protease. Within the ClpXP enzyme, ClpX recognizes, unfolds and translocates substrates into the degradation chamber of ClpP where the substrate is processed into short peptides. Because of its destructive power, ClpX must select substrates with exquisite precision to ensure proper substrates are chosen, and unfolding specifically occurs at the proper stage in a biochemical pathway. The sequences, affinities and organization of recognition signals used for different classes of ClpX substrates is being actively investigated.

Proteins targeted for ClpXP degradation or ClpX disassembly are recognized via short peptide sequences. These recognition signals, or tags, are often located near the termini of otherwise native substrate proteins[5,6]. Examples of substrates with N-terminal recognition tags are a protein that binds the phage λ origin of DNA replication (λO) and a subunit of a DNA repair/tolerance polymerase (UmuD)[7,8]. A well-characterized ClpX C-terminal signal is the 11-residue ssrA tag, which marks incompletely translated proteins from stalled ribosomes for degradation by ClpXP[9]. Some substrates have multicomponent recognition signals. Studies that identified ClpXP substrates *in vivo* revealed that numerous proteins carry multiple ClpX-recognition sequences and that many substrates were subunits of homomeric or heteromeric complexes [10,11]. Thus, we are interested in understanding mechanistically how ClpX recognizes multi-protein complexes for remodeling or disassembly.

ClpX is a homohexamer. Each subunit contains three domains; the N-terminal zinc-binding domain (N-domain) and the large and small domains characteristic of the AAA+ ATPase fold [2,4]. The ATPase domains of six subunits assemble into a donut-shaped complex with a central pore that binds the specific peptide tags on substrates and contains critical components of the active center for ATP-driven protein unfolding and translocation (*e.g.* the conserved pore loops). The N-domain forms dimers such that there are three N-domain dimers in a ClpX hexamer[12,13]. These N-domains bind auxiliary recognition peptides are present on adapter proteins or within some substrates; binding of these recognition-peptides to the ClpX N-domain enhances recognition of specific substrate proteins.

To investigate how ClpX specifically recognizes multi-protein complexes and does so at the proper step in a biological pathway, we used MuA transposase as a substrate. Phage Mu

[1]Abreviations: AAA+, ATPases associated with various cellular activities superfamily; STC, Strand transfer complex; CDC, cleaved donor complex; C-tag, C-terminal recognition tag; E-tag, enhancement recognition tag

duplicates its genome by replicative transposition, a process in which MuA binds DNA sites at the ends of the Mu genome, forms a tetramer that brings the two ends of the phage DNA together, and catalyzes the DNA cleavage and joining reactions necessary for transposition [14–16]. These recombination steps of transposition are driven forward because each reaction step generates an increasingly stable nucleoprotein complex (transpososome). The final recombination complex is the hyperstable DNA product-bound transpososome (the strand transfer complex or STC)[17]. Remodeling by ClpX then converts this hyperstable MuA-DNA complex into a fragile complex, which facilitates MuA disassembly, release of the DNA, and recruitment of DNA-replication machinery[18–20]. Completion of the later stages of replicative transposition therefore requires that the stable, terminal STC be remodeled by ClpX. Genetic studies confirm that ClpX is essential for Mu growth, whereas ClpP is clearly dispensable[21]. Thus, the unfolding activity of ClpX is important for the Mu life cycle, rather than the protease activity of ClpXP.

Although both monomeric and DNA-bound tetrameric MuA are substrates of ClpX, the STC transpososomes are the highest-priority target. Thus, we sought to understand how preferential recognition and remodeling of this specific complex is achieved. Previous studies revealed that information in the C-terminal domain of MuA (domain IIIβ) plays a central role in guiding ClpX recognition. A tag at the very C-terminus of domain IIIβ (RRKKAI-COOH; termed “C-tag”) binds in the ClpX pore and is necessary for ClpX recognition of both monomeric MuA and of transpososomes[18,22,23]. However, transpososome recognition requires more than simply the avidity afforded by four C-tags. Efficient disassembly by ClpX was inferred to require additional sequence elements within MuA’s domain IIIβ based on the defect in disassembly resulting from three specific point mutations in this domain[23]. Furthermore, the N-domain of ClpX is critical for transpososome remodeling but plays little role in MuA monomer degradation[23]. Domain IIIβ of MuA transposase contains another regulatory region that interacts with the target DNA-delivery protein MuB. Interestingly, the site of MuB interaction at least partially overlaps with the C-tag recognized by ClpX, and MuB is an antagonist of the ClpX-transpososome interaction[22]. Despite being a key regulatory domain, there is no high-resolution structure of domain IIIβ. This region is predicted to be largely disordered, with some helical structure near the C-terminus[24]. Nonetheless, the low-resolution EM structure[25] of the transpososome and the crystal structure of the STC[26] constructed with MuA variants that contained the C-terminal domain through domain IIIα, help to constrain where domain IIIβ may lie within the STC.

Here, we define a specific domain IIIβ sequence as an enhancement or “E-tag” signal and demonstrate that this sequence is recognized by the N-domain of ClpX. To determine how the structure and geometry of the STC modulates ClpX recognition and activity, we designed a hybrid protein with novel DNA-binding specificity to control the location of subunits within assembled complex. This analysis reveals that efficient disassembly of STCs requires ClpX interaction with a minimum of three tags (one C-tag and two or more E-tags) distributed among the subunits of the MuA tetramer. Finally, replacing the natural C-tag of MuA with a high-affinity ClpX-targeting tag overrides the need for E-tags. These studies establish that preferential targeting of assembled MuA tetramers requires at least three

distinct contacts between MuA and ClpX and reveal key features of recognition sequences likely to be common in the specific biological recognition of multimeric protein complexes.

RESULTS

Identification of a region critical for enhanced recognition of transpososomes by ClpX

MuA transpososome assembly, recombination of DNA, and remodeling by ClpX have been reconstituted *in vitro*. MuA is a monomer in solution but assembles efficiently into STC transpososomes *in vitro*[17]. We generated STCs by incubating MuA with supercoiled plasmid DNA containing "right" and "left" DNA binding sites for MuA (Fig. 1a)[27]. Under the conditions used, attack on a target DNA proceeds rapidly after an active MuA tetramer is formed on the donor plasmid, and the target site used is usually another location on the same plasmid (*i.e.* transposition is largely intramolecular)[28]. On a native agarose gel, stable STC transpososomes (asterisk) migrates more slowly than the supercoiled substrate plasmid (black arrow in Fig.1b & 1c). In contrast, the fragile complex is unstable during electrophoresis, and the liberated DNA transposition products are visible as a characteristic series of topoisomers (Fig. 1b & 1c). To quantify the rate and extent of ClpX remodeling, we measured appearance of the fastest running topoisomer (white arrow) of the recombination products. Migration of this specific product is rapid, as it is the only product isomer that constrains supercoils from the substrate miniMu plasmid[29]. Using this species as the remodeling product insured that we specifically measured ClpX activity against STC transpososomes that had successfully completed the recombination phases of Mu transposition.

MuA is a multi-domain protein (Fig. 2a) and belongs to the DDE family of transposases and integrases (reviewed in 22–24). The majority of the structure of MuA is known, including the architecture of the transpososome [26,33–35], but there is little structural information about domain IIIβ, which contains the C-tag and three arginine residues that appear to participate in transpososome-specific contacts with ClpX [23]. To search domain IIIβ for the specific sequence element(s) important in recognition by ClpX, we mutated blocks of residues near suspected interaction regions to aspartic acids (^{617}IVG→DDD; ^{620}IF→DD; ^{623}PS→DD; ^{625}GN→DD; ^{654}IL→DD, and ^{656}EQN→DDD) surrounding a previously mutated ^{622}R→A residue[23]. We used nonconservative Asp substitutions because acidic residues disrupt ClpX interactions with other recognition tags in contrast to Ala, which often binds ClpX well[36]. The rate that ClpXP degraded MuA monomers and their variants was determined (Fig. 2c). Furthermore, after assembly into stable STCs, the efficiency of remodeling by ClpX was also quantified (Fig. 2b). These experiments were performed at substrate concentrations significantly below the apparent K_M of ClpX for wild-type transpososomes[23]. The ^{620}IF→DD mutation had dramatic effects on both degradation and disassembly by ClpXP, the ^{622}R→A and ^{623}PS→DD mutations had major effects on disassembly but not degradation, and the remaining mutations had small effects on both reactions (Fig. 2d). Thus, residues 620–624 (called the E-tag hereafter) appear to function as a peptide signal that enhances STC recognition by ClpX.

To quantify how mutations in the E-tag affect the interaction between STCs and ClpX, we assayed rates of disassembly of complexes constructed with either wild type or

the ^{623}PS→DD MuA variant at different concentrations of ClpX. Because of technical difficulties of obtaining STCs in high concentration, we determined the disassembly rate constants from single-turnover kinetics. The apparent rate (k_{obs}) was calculated at each ClpX concentration from the semilog plot (Fig. 3a). Values for k_{obs} were then plotted as a function of ClpX (Fig. 3b). These data were fit (as described in 21 and 29) to determine the enzyme concentration needed to achieve half-maximal velocity (apparent K_M) and the disassembly rate at saturating enzyme concentrations (apparent V_{max}). We used the terminology of apparent K_M ($^{app}K_M$) and apparent V_{max} ($^{app}V_{max}$) even though the reaction pathway describing disassembly of STCs does not fulfill the standard assumptions of Michaelis-Menten equation; nonetheless, they provide reproducible, valuable terms useful in comparing the impact of various MuA or ClpX mutants on disassembly. Compared to STCs consisting of all wild-type MuA, disassembly of ^{623}PS→DD MuA complexes had a five-fold slower maximal velocity and required 8-fold higher concentrations of ClpX to achieve 50% of this maximal rate. Thus the ^{623}PS→DD mutations in MuA impact both initial ClpX recognition of STCs as well as a subsequent step(s) important for disassembly (see Discussion).

The MuA E-tag interacts with the N-domain of ClpX

Efficient disassembly of Mu STCs requires the ClpX N-domain[23], which is a docking site for specific peptide signals in some substrates and adaptor-substrate complexes. For example, a peptide in the SspB adaptor binds to the N-domain of ClpX and thereby tethers specific substrates to ClpXP to enhance their degradation [38–41]. Thus, we reasoned that the E-tag in one or more MuA subunit(s) might bind to the N-domain of ClpX, providing adaptor-like contacts to enhance recognition specifically of STCs. Indeed, we detected weak binding (K_D ~380 μM) between the purified ClpX N-domain and a fluorescein-labeled peptide carrying the E-tag (MuA residues 614–633) by fluorescence anisotropy (Fig. 4a). Importantly, when we changed the ^{622}RPS sequence in the synthetic peptide to DDD, N-domain binding was reduced by at least a factor of 10 (Fig. 4a). These results strongly support the hypothesis that the E-tag makes weak adapter-like contacts between MuA and the N-domain of ClpX.

The C-tag of MuA is an intrinsically poor ClpX signal

MuA monomers are degraded by ClpXP with a $^{app}K_M$ of ~10 μM[23], whereas a peptide substrate carrying just the minimal C-tag of MuA is degraded with a $^{app}K_M$ of ~70 μM[42]. We measured the degradation tag efficiency of this MuA C-tag by fusing a short peptide containing the last ten residues of MuA (LEQNRRKKAI) to the C-terminus of the N-terminal domain of the λcI repressor (λNcI-Mu$^{C\text{-}tag}$). This fusion protein was degraded by ClpX with an $^{app}K_M$ of ~90 μM (Fig. 4b). These results demonstrate that the native MuA C-tag is a feeble ClpX recognition signal when acting in isolation. In contrast the STC is remodeled by ClpX with an $^{app}K_M$ of ~1 μM (Fig. 3b). Previous studies establish that transpososomes containing only one MuA subunit bearing a C-tag are efficiently remodeled by ClpX [23,43]. Thus, the additional ClpX contacts present in MuA, and especially in the STC, dramatically enhance recognition; the cohort of tags displayed by the STC produce a strong “composite remodeling signal” between the transpososome and ClpX. In the

experiments presented below, we address how, within the architecture of MuA complexes, the E-tags contribute to recognition and remodeling by ClpX.

Step-wise loss of E-tags weakens ClpX affinity for complexes

Biochemical and structural studies have shown that there are two different classes of subunits within the MuA tetramer[25,26,44]. The Mu transpososome structure shown in Fig. 5a has 2-fold symmetry around its vertical axis, but the upper and lower subunits adopt different conformations. Note that tetramers for structural studies were formed using two identical DNAs that mimic the phage right end, but such complexes are highly active *in vitro* and expected to be structurally similar to those formed with natural left and right ends[26,45]. The active sites of the catalytic class-1 subunits (green in Fig. 5a) are positioned for DNA cleavage and strand transfer (the DNA ligation activity catalyzed by MuA during transposition). In contrast, the active sites of the class-2 subunits (purple and pink in Fig. 5a) face solvent and are far from any DNA. We sought to determine how the positions of MuA subunits in the transpososome affect the ability of their E-tags to enhance recognition and activity of ClpX against the Mu STC.

To assay the E-tag contributions of individual subunits, we engineered a chimeric MuA variant that facilitated assembly of complexes with a defined mixture of wild-type and mutant subunits. For subunit-specific mutations we improved upon a strategy of creating a variant MuA protein with distinct binding specificity[46]. The transpososome structure suggested that the sequence-specific DNA binding domains (Iβ and Iγ) of the class-2 subunits could be swapped for heterologous DNA binding domains because they make no protein-protein contacts within the tetramer (Fig. 5a). We therefore constructed a “SinMu” chimera comprised of the DNA-binding domain from Sin resolvase (residues 147–200), which recognizes a DNA sequence distinct from MuA[47,48], covalently joined to domains II and III of MuA (residues 253–663) via a short flexible polypeptide linker (Fig. 5b). We also constructed an altered-specificity DNA substrate from a parental mini-Mu plasmid (see *Materials and methods*). The resulting DNA (pSinRRSin) carried symmetrical protein binding sites on the left and right ends of the “mini Mu transposon” sequence with native MuA-binding sites for each of the two catalytic (class-1) subunits and Sin-DNA binding sites for each of the two structural (class-2) subunits (Fig. 5c). Assembly of mixed subunit STCs with the pSinRRSin plasmid depended on the presence of both MuA and SinMu proteins (Fig. 5d, lane 6); these data reveal that these mixed subunit transpososomes were fully competent to assemble stable complexes and carryout the DNA cleavage and joining reactions needed for transposition. In contrast no stable complex formation or catalytic activity was detected in reactions containing either MuA or SinMuA alone (Fig. 5d, lanes 2–5). We conclude from these mixing experiments, that the Sin-DNA sites position SinMu subunits to become the class-2 subunits whereas two subunits of wild type MuA become the class-1 subunits in these transpososomes.

ClpX disassembled mixed subunit STCs (with two WT MuA subunits and two SinMuA subunits) efficiently when all four subunits carried wild-type domain IIIβ, with intact E-tags and C-tags. The $^{app}K_M$ for disassembly was ~1.3 μM and an $^{app}V_{max}$ was 3.0 min^{-1} (Fig. 6a, black). These kinetic parameters are very similar to the values for disassembly of native

MuA STCs (Fig. 3b), indicating that the presence of the Sin DNA-binding domain does not significantly alter ClpX's ability to remodel the complexes. In contrast, with this hybrid DNA substrate (pSinRRSin), ClpX disassembly of transpososomes assembled with a mixture of SinMuA and MuAΔC8 subunits was barely detectable (Fig. 6a, gray). As the MuAΔC8 protein can only occupy the class-1 position of our hybrid substrate, this result agrees with earlier experiments (not using SinMu) which established that efficient ClpX recognition of an STC requires at least one class-1 subunit to have a functional C-tag[49,50].

We also assayed ClpX disassembly of transpososomes bearing the ^{623}PS→DD E-tag mutations in class-1 subunits ($^{app}K_M$ ~4.5 μM), class-2 subunits ($^{app}K_M$ ~4.4 μM), or all four subunits ($^{app}K_M$ ~11.5 μM) (Fig. 6b). These data reveal that E-tags in both catalytic subunits and structural subunits of the STC contribute to its recognition by ClpX. The $^{app}V_{max}$ for transposome disassembly was also reduced by E-tag mutations in both types of subunits, albeit to different extents, indicating that post-recognition steps in STC remodeling are also hampered by removal of functional E-tags. Interestingly, having fully functional E-tags on the class-2 subunits was more important for ClpX to engage a class-1 subunit for unfolding. These data show a benefit the assembled complex imparts to the ClpX remodeling reaction since interaction with both a class-1 and a class-2 subunit is needed to achieve the more rapid unfolding/remodeling events (see Fig. 8 and discussion).

Transpososomes with a strong C-tag do not require E-tags for efficient disassembly

Our results support a model in which the sequences throughout the Mu STC transpososomes serve as "auto-adapters" for ClpX recognition. By this model, the E-tags of MuA, like an adapter, enhance ClpX's affinity and activity for a substrate with a weak intrinsic pore-binging tag, such as the weak C-tag of MuA. To test if the function of the four E-tags would be bypassed if the MuA C-tag was replaced by a C-tag with a much tighter affinity for the ClpX pore, we constructed a MuA variant in which the C-tag was replaced with an ssrA tag (MuA$^{\Delta C\text{-tag}}$ssrA; Fig. 7a). The $^{app}K_M$ for ClpX disassembly of STCs composed of MuA$^{\Delta C\text{-tag}}$ssrA subunits with wild-type E-tags (1.6 ± 0.2 μM) was only marginally tighter than for STCs constructed with MuA$^{\Delta C\text{-tag}}$ssrA subunits with ^{623}PS→DD E-tags (2.1 ± 0.3 μM) and both values were close to that determined for wild-type MuA complexes (1.4 ± 0.2 μM) (Fig. 7b). We conclude that the E-tag is unnecessary for efficient transposome recognition in the context of a high-affinity C-tag. It was also clear that ssrA-tagged STC transpososomes were remodeled much faster than native complexes, indicating the sequence identity of the C-tag, and the presence or absence of E-tags influences both the initial affinity of ClpX for the STC as well as subsequent step(s) in catalysis of remodeling (Fig. 7b; see Discussion). Furthermore, ClpXP degraded MuA$^{\Delta C\text{-tag}}$ssrA monomers with an apparent K_M of 1.6 ± 0.4 μM (Fig. 7c), a very similar value as measured for recognition of the ssrA-tagged STCs. Thus, we conclude that the tight-binding C-tag on transpososome subunits causes ClpX to lose its ability to preferentially recognize assembled STCs compared to monomers of MuA.

DISCUSSION

MuA transposase carries two distinct types of ClpX-interacting sequences (called tags). Here we identify and define the characteristics of the primary enhancement tag (E-tag) in domain IIIβ of MuA as well as furthering the understanding of MuA's C-terminal pore-binding tag. We find that both classes of tags are intrinsically weak (E-tags, K_D> 300μm, C-tag $^{app}K_M$~ 70 μM). However, when one C-tag is recognized with the assistance of two or more E-tags distributed among the subunits of the MuA tetramer, together they constitute a composite recognition signal with an $^{app}K_M$ of approximately 1 μm, substantially tighter than any of the tags acting alone and also tighter than unassembled MuA monomers. Furthermore, the manner in which these two classes of tags are distributed among the multiple subunits of MuA lays the foundation for elucidating how ClpX may be guided to preferentially attack the end-stage MuA-tetramer-DNA complex (the STC), where ClpX unfolding is essential for phage replication and propagation (see below).

The C-tag of MuA, comprised of the ~ 8 C-terminal residues (QNRRKKAI), has long been known to be essential for ClpX to recognize and process both tetrameric and monomeric MuA[18]. Here we establish that, although it is an essential part of the MuA STC's composite recognition signal, when acting in the absence of E-tags, MuA's C-tag is weak ($^{app}K_M$ of ~90 μM) and also supports a comparably slow maximal degradation rate of only ~3 molecules per minute per $ClpX_6$ (Our groups commonly report V_{max} values normalized to the total enzyme concentration, to facilitate direct comparison between different experiments; the term *kcat* is avoided as we do not know the functional number of active sites in our enzyme.) We argue that the fact that MuA carries such a weak intrinsic C-tag for ClpX protein-processing pore is a key signal feature that allows ClpX recognition and unfolding to be controlled by MuA's assembly state as well as by the stage of the recombination pathway.

The apparent K_M for STC disassembly by ClpX is substantially tighter than the K_M for MuA monomer degradation by ClpXP [23]. In both cases, a single C-tag is likely to be engaged by ClpX, and thus differences in ClpX E-tag interactions, as well as accessibility of an exposed C-tag on a class-1 MuA subunit almost certainly explain most or all of the preference of ClpX for the STC transpososome compared to MuA monomers. The simplest possibility is that two or more of the three N-domain dimers in the ClpX hexamer engage two or more E-tags in the assembled STC, whereas only one such interaction would be possible in MuA monomers. Moreover, the geometry and thus energetic coupling between C-tag and E-tag binding is likely to be very different in tetrameric transpososomes than monomers. Most E-tag mutations we characterized have small effects on degradation by ClpXP, suggesting that the mutated residues play little role in monomer recognition. For example, the ^{622}R→A and ^{623}PS→DD mutants were degraded at 75–95% of the wild-type rate but were disassembled at 10–15% of the wild-type rate. By contrast, the ^{620}IF→DD mutant was degraded at approximately 15% of the wild-type rate and disassembled at about 5% of the wild-type rate. Thus, during monomer recognition, ClpX appears to interact with at least part of our newly identified E-tag.

The nature and geometry of interactions between adaptor-like tags and ClpX can have substantial effects on the maximal rate of ClpXP degradation[3,51]. For transpososome disassembly, we find that the ^{623}PS→DD mutation reduces the maximal rate of ClpX disassembly approximately 5-fold and weakens (increases) the $^{app}K_M$ substantially. This result can be understood if transpososome-ClpX contacts in the ^{623}PS→DD mutant are dynamic (Fig. 8). For example, weakened E-tag interactions in complexes of this MuA variant (^{623}PS→DD) with ClpX might result in the C-tag only being engaged part of the time by ClpX (Fig. 8b). This model can also explain why replacing the native C-tag of MuA with the ssrA tag both eliminates the need for the E-tag and increases the maximal disassembly rate substantially (Fig. 8c). Specifically, we envision that in ClpX complexes with transpososomes bearing the ssrA tag, this tight-binding tag is engaged by the axial pore of ClpX essentially constantly, eliminating the need for E-tag assistance because the C-tag already achieves its maximum level of binding and engagement. By contrast, in ClpX complexes with transpososomes bearing the wild-type C-tag of MuA, this weak-binding tag might be engaged by the axial pore only 20% of the time with wild-type E-tag assistance, and only 4% of the time with ^{623}PS→DD mutant E-tags. From a biological perspective, slowing the rate of transpososome disassembly by utilizing a weak C-tag could prevent ClpX disassembly of MuA-DNA complexes that had not completed recombination and also cause the preferential recognition of transpososomes, especially STCs (see below and Fig. 7), while minimizing ClpXP degradation of unassembled MuA subunits.

For many ClpX substrates, we consider the $^{app}K_M$ as a useful approximation of the binding affinity between ClpX and it's substrate. For transpososome disassembly, we observe that mutations of the E-tag reduce the maximal velocity up to 5-fold. This unexpected finding reveals that E-tags contribute to the initial substrate-enzyme interaction and to a downstream step, which we have denoted as "engagement" in our model (Fig.8). The engagement step may be interpreted as a commitment by ClpX to translocate the bound polypeptide. In wild-type transpososomes, E-tags may enhance the engagement/commitment of the weak C-tag; this engagement step should be principally expressed in the reaction's *Vmax*. Without E-tags, the commitment step is slowed and this suppression of engagement is manifested as a slower $^{app}V_{max}$ (Fig 8b). Characterization of the enzyme-substrate contacts and the kinetic contributions of "engagement" has been difficult using bulk assays with simple single-domain proteins. However, recent experiments with multi-domain substrates, pre-engagement protocols and single molecule optical trap experiments are allowing isolation of initial recognition and engagement into distinct steps. Although these approaches are not yet readily applied to transpososome remodeling, we are observing distinctions between these two steps and evidence that weaker engagement is expressed in a slower $^{app}V_{M.}$ These observations are consistent with the behavior seen in this study where the strong ssrA C-tag is efficiently engaged whereas the weaker MuA C-tag is engaged less readily, resulting in a slower V_{MAX} and the opportunity to have this velocity enhanced by the E-tags.

The architecture of the Mu transpososome restricts how the C-tags and E-tags of the two catalytic and two structural MuA subunits could interact with the pore and N-domains of ClpX. E-tags in both types of MuA subunits can interact with ClpX, whereas the C-tags can only be donated from the catalytic ("class-1") subunits during ClpX recognition[45,49,50].

Simple modeling suggests that ClpX could span the C-terminal regions of the two catalytic subunits in the STC (Fig. 9a). Furthermore ClpX also appears able to reach the C-terminal terminal regions of a catalytic subunit and a structural subunit on the same side of the axis of symmetry, or the C-terminal regions of a catalytic subunit and a structural subunit on opposite sides of the axis of symmetry. Either model that involves both a catalytic subunit and a structural subunit is consistent with our experimental observations. By making the E-tag accessible on all four subunits, the architecture of the transpososome maximizes the permutations for successful recognition. Having E-tags in multiple subunits accessible to ClpX is also likely to be beneficial as the MuB regulatory protein also binds the C-terminal region of subunits in Mu transpososomes, and ClpX might make initial contacts with some MuA subunits in a complex prior to the exit of the dimeric MuB from the same complex.

An attractive model for ClpX interaction and attack on the STC is proposed in Fig. 9b, which takes its foundations from the dynamic interaction results presented here, in context with the recent Mu transpososome structure, and the insights regarding how domains must reorient during the multiple steps of the recombination process. The structure strongly implies that domain III of the class-1 subunits must move upon target binding. The MuA variant used for structure determination ended with domain IIIα (residues 575–605). This domain IIIα region forms a long, positively charged, amphipathic helix. Consistent with biochemical analyses[52,53], domain IIIα of the class-2 subunits appears integral to the stability of the complex and may not move after initial complex assembly. However, in the class-1 subunits, two copies of domain IIIα pair between the arms of the bent target DNA, presumably electrostatically stabilizing the DNA conformation. These domain IIIα regions must adopt this clamped down conformation only after the target DNA has bound, as they would otherwise block its access to the transpososome active site. We propose that the optimal arrangement of ClpX recognition tags is only achieved after target DNA binding. Movement of domain IIIα from the class I subunits into the central cleft would necessarily reposition the rest of domain IIIβ and its ClpX recognition tags.

The use of multivalent recognition signals, some interacting with the axial pore and some with auxiliary domains, is a common theme in substrate recognition by AAA+ unfolding and remodeling enzymes. The bacterial cell-division protein, FtsZ, was recently shown to contain two sites important for proteolysis by ClpXP. Similarly to MuA, FtsZ contains a C-terminal tag and an internal recognition element located 30 residues from the C terminus[54]. The bacterial AAA+ ClpV unfoldase disassembles VipA/VipB tubules of the type-VI secretion system in many pathogenic proteobacteria, and multiple interactions between ClpV and VipA/VipB tubules result in an enzymatic preference for assembled VipA/VipB complexes over VipB monomers[55]. Recognition of ubiquitin-tagged substrates by the 26S proteasome also involves multivalent signals. A poly-ubiquitin tag can mediate proteasome binding, but the tagged protein is not degraded unless it has an unstructured region that can be engaged by the AAA+ Rpt subunits that form the hexameric protein-unfolding ring in the 19S cap[56–58]. This multivalent recognition strategy parallels ClpX recognition of Mu transpososomes. One signal is engaged by the axial pore of the AAA+ enzyme (unstructured regions of proteasomal substrates or the C-tag of MuA), and the second signal is recognized by an auxiliary domain or subunit (ubiquitin binding to the Rpn13 receptor or E-tag binding to the N-domain of ClpX). It will be interesting to continue examining how the relative

strengths of different signals that bind remodeling and degradation enzymes regulate recognition of a protein or multi-protein complex.

Materials and Methods

Buffers

Buffer L1, W20, W250 contained 25mM HEPES-KOH pH 7.6, 100mM KCl, 400mM NaCl, 10mM beta-mercaptoethanol, 10% glycerol, and Imidazole at concentrations of 10mM, 20mM, and 250mM, respectively.

Buffer S300 and S1000 contained 25mM HEPES-KOH pH 7.6, 0.1mM EDTA, 1mM DTT, 10% glycerol, and KCl at concentrations of 0.3M and 1M, respectively.

PD50 buffer contained 25mM HEPES-KOH pH 7.6, 50mM KCl, 5mM MgCl2, 0.032% NP-40, 10% glycerol.

Buffer LM, LM20, LM250 contained 10mM Tris-Cl pH 8, 100mM NaCl, 1mM DTT, 10% glycerol, and imidazole at concentrations of 10mM, 20mM, and 250mM, respectively.

Buffer S50 and S500 contained 50mM Tris-Cl pH 8, 1mM DTT, 10% glycerol, and NaCl at concentrations of 50mM and 500mM, respectively.

Protein and peptide purification

Wild-type and mutant variants of MuA proteins[28], *E. coli* ClpX [59], HU [60], ClpP [61], ClpXΔN (residue 47–424) [23], N-domain of ClpX (residue 1–64) with a cleavable N-terminal His6 tag [62] were purified as previously described.

Construction and optimization of SinMu—SinMu, the construct used in the experiments reported here, is comprised of (in order): an N-terminal His6 tag, Sin residues 147–200, a ten-residue SG repeat, and residues 253–663 of MuA.

The initial Sin-Mu chimera construct, termed Sin5Mu, was the same except the interprotein linker was only 5 amino acids and the MuA portion comprised only residues 258–605. Sin5Mu was cloned using sticky-end PCR cloning[63]. Two sets of PCR were initially performed. The first reaction utilized primers that would amplify the DNA encoding Sin 147 to 200 with a 3′-terminal extension that includes the linker and the first 15 base pairs from the MuA construct. The second reaction utilized primers that would amplify the DNA encoding MuA 258 to 605 with a 5′-terminal extension that starts with the last 15 base pairs from the Sin construct followed by the linker. The PCR products from these two reactions were then combined to serve as a template in the next round of PCR. This round involved two sets. The first set utilized 5′TATGGGACGACCTTTGCTTTATTCACCG and 5′-CTTACGGCAGCAGCTCTGCCACTTCC, and the second set utilized 5′-TGGGACGACCTTTGCTTTATTCACCG and 5′-GATCCTTACGGCAGCAGCTCTGCCACTTCC for their respective forward and backwards primers. These primers were designed such that when the top strand of the first PCR product anneals with the bottom strand of the second product, it will form a DNA with

overhangs that mimic a DNA that has been cleaved with NdeI and BamHI. Product from these two reactions were therefore combined, boiled for five minutes, and annealed at room temperature. This newly annealed DNA was then ligated to pET3a that has been treated with NdeI and BamHI. The sequence was verified with the University of Chicago DNA Sequencing Facility, and contained only one amino acid change, T504A. T504 is surfaced-exposed, and A is the WT residue in the nearly-identical D108A protein [64]. To test the activity of Sin5Mu, we carried out *in vitro* strand transfer reactions using pUC19 as target DNA, equimolar mixtures of Sin5Mu and WT $MuA_{77–605}$, and donor DNA duplexes that carried the R1 MuA binding site and the Sin binding site juxtaposed as suggested by molecular modeling, as well as spaced +/− 1 and +/− 2 bp from the modeled optimum. Activity was only seen on the −1 donor DNA. This result suggested that the chimera might be more active if the spacer were longer.

Additional chimeras with longer linkers were made using QuikChange (Stratagene). Sin10Mu contains additional GSGSG linker. Sin15Mu and Sin20Mu are essentially Sin10Mu but with Mu constructs starting at residues 253 and 248, respectively. All four Sin-Mu chimeras were then tested against 2 donor DNAs: the −1nt spacing between binding sites that was experimentally optimal for Sin5Mu, and that expected to be optimal from modeling. Lengthening the amino acid spacer between the two protein domains clearly improved the yield of the strand-transfer product. Although Sin5Mu and Sin10Mu still preferred the −1 spacing between recognition sites, Sin15Mu and Sin20Mu did not discriminate. All further work was based on the Sin15Mu construct and the −1 spacing in the donor DNA sequence.

The remainder of domain III was appended to create SinMu, the construct used in these studies. pSinMu was cloned from plasmid pSin15Mu by appending the remaining MuA transposase sequence such that the construct ends at the natural C-terminus of MuA, (residue 663), using Quickchange to remove an internal BamHI site, and inserting into pET3a vector via its NdeI and BamHI restriction sites.

Purification of SinMu—pSinMu was transformed into *E. coli* strain BL21(DE3). Cells were grown at 37°C to OD_{600nm} ~ 0.6 in Luria-Bertani broth containing 100 μg/mL ampicillin. Protein expression was induced for 3 hours by addition of 0.4mM IPTG. The culture was harvested by centrifugation, resuspended in 10mL of BufferL1 per liter of initial cell culture, and lysed by French press. The lysate was treated with PMSF, cleared by centrifugation for 30min at 30,000×g 4°C and incubated with Ni- NTA agarose beads equilibrated in BufferL1 for 1 hour at 4°C. The beads were transferred to a column, washed with Buffer W20, and bound protein was eluted using Buffer W250. Fractions containing SinMu variants were identified by SDS-PAGE, buffer-exchanged into Buffer S300 using PD-10 desalting columns. The eluate was further purified by anion exchange chromatography, MonoS equilibrated with Buffer S300, and eluted by gradient to Buffer S1000. Fractions containing SinMu variants were identified by SDS-PAGE, pooled, and concentrated using Amicon (MWCO 5k) filter tubes, and the protein concentration by determined by Bradford reagent.

MuΔ8ssrA was generated from pTB1, a pET3d containing MuA transposase. The last eight Cterminal residues were replaced with the sequence for ssrA tag, generated by PCR with 5′-phosphate primers:

LLO62: aactacgctttagcagctTAAGGATCCGGCTGCTAACAAAGCC and

LLO63: ttcgtcgtttgcggcTTCCAGAATATCCAGCGAATGATTCAGATA.

The variant MuΔ8ssrA (P623D S624D) was cloned by PCR using 5′-phosphate primers

LLO64: gaTgaCGGTAATACGGAACGGGTGAAG and

LLO55: CCGGAAAATACCAACAATTCGTGA. Both MuΔ8ssrA and MuΔ8ssrA (PS/DD) proteins were expressed and purified using the protocol for wild-type MuA.

Strain TB352 contains pET28b: λ-cI-MuA comprised of residues 1–93 of lambda cI repressor, followed by FLAG-His6 tag, a linker and residues 654–663 of MuA. The plasmid was transformed into *E. coli* strain BL21(DE3). Cells were grown at 37°C to OD_{600nm} ~ 1.0 in Luria-Bertani broth containing 100 μg/mL kanamycin, harvested and transferred to M9+10% v/v LB media containing antibiotic, then grown at 37°C for another hour. Protein expression was induced for 3 hours by addition of 0.4mM IPTG. 20min after IPTG addition, cultures were spiked with 2mCi EasyTag EXPRESS protein labeling mix (PerkinElmer). The culture was harvested by centrifugation, resuspended in 2mL of Buffer LM per 100mL of initial cell culture, and lysed by lysozyme in four freeze/thaw cycles. Lysate was incubated with benzonase nuclease and protease inhibitor cocktail III for 1 hr, cleared by centrifugation for 30min at 21,000xg 4°C and incubated for 1 hour at 4°C with Ni-NTA agarose beads equilibrated in BufferLM. The beads were transferred to a column, washed with Buffer LM20, and bound protein was eluted using Buffer LM250. Elution fractions were buffer exchanged into Buffer S50. The eluate was further purified by anion exchange chromatography, MonoS equilibrated with Buffer S50, and eluted by gradient to Buffer S500. Fractions containing λ-cI-MuA were identified by SDS-PAGE, pooled and concentrated using Amicon (MWCO 5k) filter tubes, and the protein concentration by determined by absorbance at 280nm.

N-λcI is a His6-SUMO followed by residues 1–93 of λ cI in pET23b. The plasmid was transformed into *E. coli* strain BL21(DE3). Cells were grown at 37°C to OD_{600nm} ~ 1.0 in Luria-Bertani broth containing 100 μg/mL ampicillin, harvested and transferred to M9+10% v/v LB media containing antibiotic, grown at 37°C for another hour. Protein expression was induced for 3 hours by addition of 0.4mM IPTG. 20min after IPTG addition, cultures were spiked with 2mCi EasyTag EXPRESS protein labeling mix (PerkinElmer). The culture was harvested by centrifugation, resuspended in 2mL of Buffer LM per 100mL of initial cell culture, and lysed by lysozyme in four freeze/thaw cycles. Lysate was incubated with benzonase nuclease and protease inhibitor cocktail III for 1 hr, cleared by centrifugation for 30min at 21,000×g 4°C and incubated for 1 hour at 4°C with Ni-NTA agarose beads equilibrated in BufferLM. The beads were transferred to a column, washed with Buffer LM20, and bound protein was eluted using Buffer LM250. Elution fractions were buffer exchanged into Buffer LM and incubated with Ulp1 enzyme overnight to cleave His6-SUMO tag. N-λcI was separated from uncleaved His-SUMO fusion protein by flowing over Ni-NTA agarose equilibrated with Buffer LM and collecting the flow through. Protein was

buffer exchanged into Buffer LM absent imidazole, and the protein concentration by determined by absorbance at 280nm.

Fluorescein-labeled peptides corresponding to MuA residues (614–633), MuA variants containing aspartate substitutions, and to SspB residues (152–162) were synthesized by FMOC technique on an Apex 396 solid-phase synthesizer and purified by HPLC on a reverse-phase C12 column running a gradient 0–100% Acetonitrile, 0.06% v/v TFA. Fractions containing fluorescein-labeled peptides were verified by MALDI-TOF mass spectrometry (MIT Biopolymer facility).

DNA for transposition

pSinRRSin was generated from miniMu plasmid, pMK586. pMK586 was digested with ClaI and EcoN1 to remove the phage left-end attachment sites, treated with Antartic phosphatase, and ligated to 5′-phosphorylated and annealed oligonucleotides (lower case denotes Sin binding motifs).

LLO37:
CCAAGGAAGCTTGAAGCGGCGCACGAAAAACGCGAAAGCcgtatgattagggtAT
and

LLO38:
CGATaccctaatcatacgGCTTTCGCGTTTTTCGTGCGCCGCTTCAAGCTTCCTTG
containing the R1-Sin binding sites with appropriate overhangs. The right-end R2 binding site was replaced with Sin binding sequence, generated by PCR with 5′-phosphate primers

LLO46: tcatacgGCTTTCGCGTTTTTCGTGCGC and

LLO47: ttagggtCTTTAGCTTTCGCGCTTCAAATG

Transpososome Assembly

Transpososomes were assembled *in vitro* in the following buffer: 25mM HEPES pH7.6, 10mM MgCl2, 15% glycerol, 0.1mg/mL BSA, 1mM DTT, 100mM NaCl, 9% DMSO. Transposition reactions contained 16μg/mL supercoiled pMK586, 130nM HU, 100nM MuA. The reaction was incubated at 30°C for 20min. To assemble SinMu chimeric transpososomes, 16μg/mL supercoiled pSinRRSin, 130nM HU, 50nM MuA variant, 50nM SinMu variant were incubated at 30°C for 60min.

Degradation Assay

ClpX and ClpP were preincubated with ATP regeneration mix for 1min at 30°C prior to addition of substrate in PD50 buffer. Final concentrations: $ClpX_6$=0.3μM, $ClpP_{14}$=0.8μM, substrate=1μM, ATP=4mM, creatine phosphate= 5mM, creatine kinase=0.05mg/mL. Samples (5μL) were removed at different times and stopped by addition of 2.5x SDS loading buffer. After SDS-PAGE, products were visualized with Coomassie Blue stain

Degradation Assay for determination of steady-state kinetic parameters

ClpX and ClpP were preincubated with ATP regeneration mix for 1min at 30°C prior to addition of S35-labeled substrate in PD50 buffer. Final concentrations: $ClpX_6$=0.3μM, $ClpP_{14}$=0.8μM, substrate= as indicated in figures, ATP=4mM, creatine phosphate= 5mM, creatine kinase=0.05mg/mL. Samples (10μL) were removed at each timepoint, added to ice cold 5uL 50% TCA and incubated on ice for 15min. Samples were centrifuged at 21000×*g* 4°C 10min. The supernatant containing TCA-soluble peptides was transferred to vials of 4mL scintillation fluid. Two samples from each reaction were added directly to scintillation fluid for upper-limit controls. Vials were counted by the Tri-Carb 2910 (Perkin Elmer). Rates of degradation were quantified by linear regression of the cpm (counts per min) normalized to specific radioactivity over time.

Disassembly Assay for determination of Steady-State kinetic parameters

ClpX was preincubated with ATP regeneration mix for 1min at 30°C prior to addition of substrate in PD50 buffer. Final concentrations: ATP 4mM, Creatine phosphate= 20mM, creatine kinase=0.25mg/mL. For each timepoint, the reaction was stopped by addition of EDTA to 50mM. Samples were electrophoresed on 0.9% High gelling temperature-agarose gel (Lonza) containing 10μg/mL BSA and 10μg/mL heparin. Gels were stained with SYBR Green I (Invitrogen) and visualized using a Typhoon imager (GE). Rates of disassembly were quantified using ImageQuant (GE) as previously described[23]. Briefly, for each time point, the DNA product band was calculated as a percent of the total pixels in the lane and normalized to the product band in the “+SDS lane”, which was used as the “100% disassembly” control.

Peptide-binding assay

Fluorescein-labeled peptides were incubated with increasing amounts of ClpX N-domain in PD50 buffer at 30°C, and fluorescence was measured using a Photon Technology International fluorimeter set up with two detectors (495nm excitation; 520nm emission). ClpX N-domain alone minimally scattered light. This background scatter was subtracted and G-factor was determined by the instrument. Anisotropy was calculated using the equation $r=\frac{I_{||}-Gfactor*I_{\perp}}{I_{||}+2*Gfactor*I_{\perp}}$. The K_D values were determined by fitting binding data to a hyperbolic equation.

Acknowledgments

This work was supported by the National Institutes of Health grants GM-49224 (to TAB), AI-16892 (to RTS), GM101989 (to PAR), and the NIH Pre-Doctoral Training Grant T32GM007287. We’d like to thank Martin Boocock for helpful discussions regarding construction of the SinMu chimera, Aliaa Abdelhakim and Briana Burton for advice and discussions, and Igor Levchenko for synthesis of peptides. TAB is an employee of the Howard Hughes Medical institute.

References

1. Snider J, Thibault G, Houry WA. The AAA+ superfamily of functionally diverse proteins. Genome Biol. 2008; 9:216. [PubMed: 18466635]
2. Wendler P, Ciniawsky S, Kock M, Kube S. Structure and function of the AAA+ nucleotide binding pocket. Biochim Biophys Acta. 2012; 1823:2–14. [PubMed: 21839118]

3. Sauer RT, Baker Ta. AAA+ proteases: ATP-fueled machines of protein destruction. Annu Rev Biochem. 2011; 80:587–612. [PubMed: 21469952]
4. Baker TA, Sauer RT. ClpXP, an ATP-powered unfolding and protein-degradation machine. Biochim Biophys Acta. 2012; 1823:15–28. [PubMed: 21736903]
5. Sauer RT, et al. Sculpting the Proteome with AAA+ Proteases and Disassembly Machines. Cell. 2004; 119:9–18. [PubMed: 15454077]
6. Varshavsky A. The N-end rule: functions, mysteries, uses. Proc Natl Acad Sci U S A. 1996; 93:12142–9. [PubMed: 8901547]
7. Gonciarz-swiatek M, et al. Recognition, Targeting, and Hydrolysis of the λ O Replication Protein by the Recognition, Targeting, and Hydrolysis of the O Replication Protein by the ClpP/ClpX Protease. J Biol Chem. 1999; 274:13999–14005. [PubMed: 10318812]
8. Gonzalez M, Rasulova F, Maurizi MR, Woodgate R. Subunit-specific degradation of the UmuD/D′ heterodimer by the ClpXP protease: the role of trans recognition in UmuD′ stability. EMBO J. 2000; 19:5251–8. [PubMed: 11013227]
9. Gottesman S, Roche E, Zhou Y, Sauer RT. The ClpXP and ClpAP proteases degrade proteins with carboxy-terminal peptide tails added by the SsrA-tagging system. Genes Dev. 1998; 12:1338–1347. [PubMed: 9573050]
10. Flynn JM, Neher SB, Kim YI, Sauer RT, Baker TA. Proteomic discovery of cellular substrates of the ClpXP protease reveals five classes of ClpX-recognition signals. Mol Cell. 2003; 11:671–83. [PubMed: 12667450]
11. Neher SB, et al. Proteomic profiling of ClpXP substrates after DNA damage reveals extensive instability within SOS regulon. Mol Cell. 2006; 22:193–204. [PubMed: 16630889]
12. Wojtyra, Ua; Thibault, G.; Tuite, A.; Houry, Wa. The N-terminal zinc binding domain of ClpX is a dimerization domain that modulates the chaperone function. J Biol Chem. 2003; 278:48981–90. [PubMed: 12937164]
13. Park EY, et al. Structural basis of SspB-tail recognition by the zinc binding domain of ClpX. J Mol Biol. 2007; 367:514–26. [PubMed: 17258768]
14. Craigie R, Mizuuchi M, Mizuuchi K. Site-specific recognition of the bacteriophage Mu ends by the Mu A protein. Cell. 1984; 39:387–94. [PubMed: 6094016]
15. Kuo CF, Zou aH, Jayaram M, Getzoff E, Harshey RM. DNA-protein complexes during attachment-site synapsis in Mu DNA transposition. EMBO J. 1991; 10:1585– 91. [PubMed: 1851088]
16. Lavoie BD, Chan BS, Allison RG, Chaconas G. Structural aspects of a higher order nucleoprotein complex: induction of an altered DNA structure at the Mu - host junction of the Mu Type 1 transpososome. EMBO. 1991; 10:3051–3059.
17. Surette MG, Buch SJ, Chaconas G. Transpososomes: stable protein-DNA complexes involved in the in vitro transposition of bacteriophage Mu DNA. Cell. 1987; 49:253– 262. [PubMed: 3032448]
18. Levchenko I, Luo L, Baker TA. Disassembly of the Mu transposase tetramer by the ClpX chaperone. Genes Dev. 1995; 9:2399–2408. [PubMed: 7557391]
19. Nakai H, Kruklitis R. Disassembly of the bacteriophage Mu transposase for the initiation of Mu DNA replication. J Biol Chem. 1995; 270:19591–19598. [PubMed: 7642646]
20. Jones JM, Welty DJ, Chem JB, Nakai H. Versatile Action of Escherichia coli ClpXP as Protease or Molecular Chaperone for Bacteriophage Mu Transposition Versatile Action of Escherichia coli ClpXP as Protease or Molecular Chaperone for Bacteriophage Mu Transposition *. J Bacteriol. 1998; 273:459–465.
21. Mhammedi-Alaoui A, Pato M, Gama M-J, Toussaint A. A new component of bacteriophage Mu replicative transposition machinery: the Escherichia coli CipX protein. Mol Microbiol. 1994; 11:1109–1116. [PubMed: 8022280]
22. Levchenko I, Yamauchi M, Baker TA. ClpX and MuB interact with overlapping regions of Mu transposase: implications for control of the transposition pathway. Genes Dev. 1997; 11:1561–1572. [PubMed: 9203582]
23. Abdelhakim AH, Oakes EC, Sauer RT, Baker TA. Unique contacts direct high-priority recognition of the tetrameric Mu transposase-DNA complex by the AAA+ unfoldase ClpX. Mol Cell. 2008; 30:39–50. [PubMed: 18406325]

24. Cole C, Barber JD, Barton GJ. The Jpred 3 secondary structure prediction server. Nucleic Acids Res. 2008; 36:W197–201. [PubMed: 18463136]
25. Yuan JF, Beniac DR, Chaconas G, Ottensmeyer FP. 3D reconstruction of the Mu transposase and the Type 1 transpososome: a structural framework for Mu DNA transposition. Genes Dev. 2005; 19:840–52. [PubMed: 15774720]
26. Montano SP, Pigli YZ, Rice Pa. The μ transpososome structure sheds light on DDE recombinase evolution. Nature. 2012; 491:413–7. [PubMed: 23135398]
27. Mizuuchi K. In vitro transposition of bacteriophage Mu: a biochemical approach to a novel replication reaction. Cell. 1983; 35:785–94. [PubMed: 6317201]
28. Baker TA, Mizuuchi M, Mizuuchi K. MuB protein allosterically activates strand transfer by the transposase of phage Mu. Cell. 1991; 65:1003–13. [PubMed: 1646076]
29. Maxwell A, Craigie R, Mizuuchi K. B protein of bacteriophage mu is an ATPase that preferentially stimulates intermolecular DNA strand transfer. Proc Natl Acad Sci U S A. 1987; 84:699–703. [PubMed: 2949325]
30. Rice PA, Baker TA. Comparative architecture of transposase and integrase complexes. Nat Struct Biol. 2001; 8:302–7.
31. Montano SP, Rice PA. Moving DNA around: DNA transposition and retroviral integration. Curr Opin Struct Biol. 2011; 21:370–8. [PubMed: 21439812]
32. Hickman AB, Chandler M, Dyda F. Integrating prokaryotes and eukaryotes: DNA transposases in light of structure. Crit Rev Biochem Mol Biol. 2010; 45:50–69. [PubMed: 20067338]
33. Clubb RT, et al. A novel class of winged helix-turn-helix protein: the DNAbinding domain of Mu transposase. Structure. 1994; 2:1041–8. [PubMed: 7881904]
34. Clubb RT, Schumacher S, Mizuuchi K, Gronenborn aM, Clore GM. Solution structure of the I gamma subdomain of the Mu end DNA-binding domain of phage Mu transposase. J Mol Biol. 1997; 273:19–25. [PubMed: 9367742]
35. Schumacher S, et al. Solution structure of the Mu end DNA-binding ibeta subdomain of phage Mu transposase: modular DNA recognition by two tethered domains. EMBO J. 1997; 16:7532–41. [PubMed: 9405381]
36. Flynn JM, et al. Overlapping recognition determinants within the ssrA degradation tag allow modulation of proteolysis. Proc Natl Acad Sci U S A. 2001; 98:10584– 9. [PubMed: 11535833]
37. Pyle AM, Green JB. Building a kinetic framework for group II intron ribozyme activity: quantitation of interdomain binding and reaction rate. Biochemistry. 1994; 33:2716–25. [PubMed: 8117737]
38. Levchenko I, Seidel M, Sauer RT, Baker TA. A Specificity-Enhancing Factor for the ClpXP Degradation Machine. Science (80-). 2000; 289:2354–2356.
39. Levchenko I, Grant Ra, Wah Da, Sauer RT, Baker TA. Structure of a delivery protein for an AAA + protease in complex with a peptide degradation tag. Mol Cell. 2003; 12:365–72. [PubMed: 14536076]
40. Song HK, Eck MJ. Structural basis of degradation signal recognition by SspB, a specificity-enhancing factor for the ClpXP proteolytic machine. Mol Cell. 2003; 12:75–86. [PubMed: 12887894]
41. Wah DA, et al. Flexible linkers leash the substrate binding domain of SspB to a peptide module that stabilizes delivery complexes with the AAA+ ClpXP protease. Mol Cell. 2003; 12:355–63. [PubMed: 14536075]
42. Barkow, SR. Massachusetts Institute of Technology. Mechanistic Studies of the AAA + Molecular Motor ClpXP. 2009. at <http://hdl.handle.net/1721.1/49741>
43. Burton RE, Siddiqui SM, Kim YI, Baker TA, Sauer RT. Effects of protein stability and structure on substrate processing by the ClpXP unfolding and degradation machine. EMBO J. 2001; 20:3092–100. [PubMed: 11406586]
44. Namgoong SY, Harshey RM. The same two monomers within a MuA tetramer provide the DDE domains for the strand cleavage and strand transfer steps of transposition. EMBO J. 1998; 17:3775–85. [PubMed: 9649447]

45. Williams TL, Jackson EL, Carritte A, Baker TA. Organization and dynamics of the Mu transpososome : recombination by communication between two active sites. Genes Dev. 1999; 13:2725–2737. [PubMed: 10541558]
46. Namgoong SY, Sankaralingam S, Harshey RM. Altering the DNA-binding specificity of Mu transposase in vitro. Nucleic Acids Res. 1998; 26:3521–7. [PubMed: 9671813]
47. Rowland S-J, Stark WM, Boocock MR. Sin recombinase from Staphylococcus aureus: synaptic complex architecture and transposon targeting. Mol Microbiol. 2002; 44:607–619. [PubMed: 11994145]
48. Mouw KW, et al. Architecture of a serine recombinase-DNA regulatory complex. Mol Cell. 2008; 30:145–55. [PubMed: 18439894]
49. Burton BM, Williams TL, Baker TA. ClpX-mediated remodeling of mu transpososomes: selective unfolding of subunits destabilizes the entire complex. Mol Cell. 2001; 8:449–54. [PubMed: 11545746]
50. Abdelhakim AH, Sauer RT, Baker TA. The AAA+ ClpX machine unfolds a keystone subunit to remodel the Mu transpososome. Proc Natl Acad Sci U S A. 2010; 107:2437–42. [PubMed: 20133746]
51. McGinness KE, Bolon DN, Kaganovich M, Baker Ta, Sauer RT. Altered tethering of the SspB adaptor to the ClpXP protease causes changes in substrate delivery. J Biol Chem. 2007; 282:11465–73. [PubMed: 17317664]
52. Baker TA, Mizuuchi M, Savilahti H, Mizuuchi K. Division of labor among monomers within the Mu transposase tetramer. Cell. 1993; 74:723–733. [PubMed: 8395353]
53. Aldaz H, Schuster E, Baker TA. The interwoven architecture of the Mu transposase couples DNA synapsis to catalysis. Cell. 1996; 85:257–69. [PubMed: 8612278]
54. Camberg JL, Viola MG, Rea L, Hoskins JR, Wickner S. Location of Dual Sites in E.coli FtsZ Important for Degradation by ClpXP; One at the C-Terminus and One in the Disordered Linker. PLoS One. 2014; 9:e94964. [PubMed: 24722340]
55. Pietrosiuk A, et al. Molecular basis for the unique role of the AAA+ chaperone ClpV in type VI protein secretion. J Biol Chem. 2011; 286:30010–21. [PubMed: 21733841]
56. Prakash S, Tian L, Ratliff KS, Lehotzky RE, Matouschek A. An unstructured initiation site is required for efficient proteasome-mediated degradation. Nat Struct Mol Biol. 2004; 11:830–7. [PubMed: 15311270]
57. Takeuchi J, Chen H, Coffino P. Proteasome substrate degradation requires association plus extended peptide. EMBO J. 2007; 26:123–31. [PubMed: 17170706]
58. Inobe T, Fishbain S, Prakash S, Matouschek A. Defining the geometry of the two-component proteasome degron. Nat Chem Biol. 2011; 7:161–7. [PubMed: 21278740]
59. Neher SB, Sauer RT, Baker Ta. Distinct peptide signals in the UmuD and UmuD′ subunits of UmuD/D′ mediate tethering and substrate processing by the ClpXP protease. Proc Natl Acad Sci U S A. 2003; 100:13219–24. [PubMed: 14595014]
60. Baker TA, Kremenstova E, Luo L. Complete transposition requires four active monomers in the mu transposase tetramer. Genes Dev. 1994; 8:2416–2428. [PubMed: 7958906]
61. Kim YI, Burton RE, Burton BM, Sauer RT, Baker TA. Dynamics of substrate denaturation and translocation by the ClpXP degradation machine. Mol Cell. 2000; 5:639–48. [PubMed: 10882100]
62. Chowdhury T, Chien P, Ebrahim S, Sauer RT, Baker TA. Versatile modes of peptide recognition by the ClpX N domain mediate alternative adaptor-binding specificities in different bacterial species. Protein Sci. 2010; 19:242–54. [PubMed: 20014030]
63. Zeng G. Sticky-end PCR: New method for subcloning. Biotechniques. 1998; 25:206–208. [PubMed: 9714877]
64. Yang JY, Jayaram M, Harshey RM. Enhancer-independent variants of phage Mu transposase: enhancer-specific stimulation of catalytic activity by a partner transposase. Genes Dev. 1995; 9:2545–55. [PubMed: 7590234]

Highlights

- AAA+ unfoldases change the conformation of substrate proteins and protein complexes.
- How specific substrates are chosen with high priority at the proper time in a reaction pathway is being studied.
- The AAA+ unfoldase, ClpX specifically recognizes two classes of recognition tags in the MuA transposase.
- Specific features of these MuA tag classes direct ClpX to the biologically important reaction path.

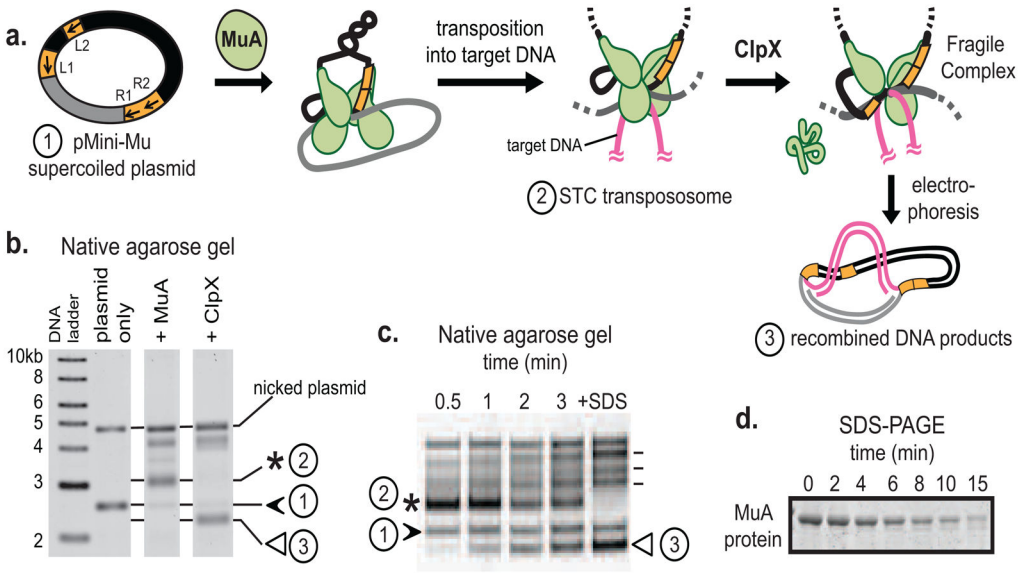

FIGURE 1. ***In vitro*** **assays for MuA complex assembly and recognition by ClpX or ClpXP**

A) MuA transposase monomers and host protein HU (not depicted for clarity) are incubated with a supercoiled plasmid substrate (1, “pMini-Mu”) containing left and right phage Mu attachment sites (L1, L2, R1, R2 are sites of stable association in the assembled complex; other sites utilized during assembly but not bound by MuA in the final STC were omitted for clarity). MuA catalyzes DNA cleavage and recombination with target DNA to form the STC transpososome (2), a stable complex. ClpX remodels the transpososome by unfolding a subunit bound to L1 or R1 attachment site to produce the fragile complex. Unlike the stable STC, the fragile complex falls apart during gel electrophoresis and liberates recombined DNA products (3).

B) On a native agarose gel, supercoiled pMiniMu runs as a band between the 2 and 3 kb linear DNA markers (1, black arrow). In the “+MuA” lane, the STC transpososome appears as a band (2, asterisk) that migrates more slowly than supercoiled plasmid alone. Addition of ClpX to reactions containing STCs produces a set of recombined topoisomers; the lowest band (3, white arrow) was quantified for disassembly rates.

C) A timecourse shows ClpX catalyzed disassembly of transposomes. Rates of MuA complex disassembly by ClpX were assayed by measuring the rate of appearance of the lowermost disassembly DNA product (3, white arrow). Addition of SDS to the reaction disrupts all inter-protein and protein-DNA interactions within the STC transpososomes and serves as the “100% disassembly” control. Other recombined DNA products are indicated by dash lines next to +SDS lane; details on these topoisomers are in Maxwell et al. *PNAS* 1987.

D) A timecourse shows ClpXP catalyzed degradation of monomeric MuA. Rates of protein degradation were assayed by measuring the rate of disappearance of MuA on SDS-PAGE

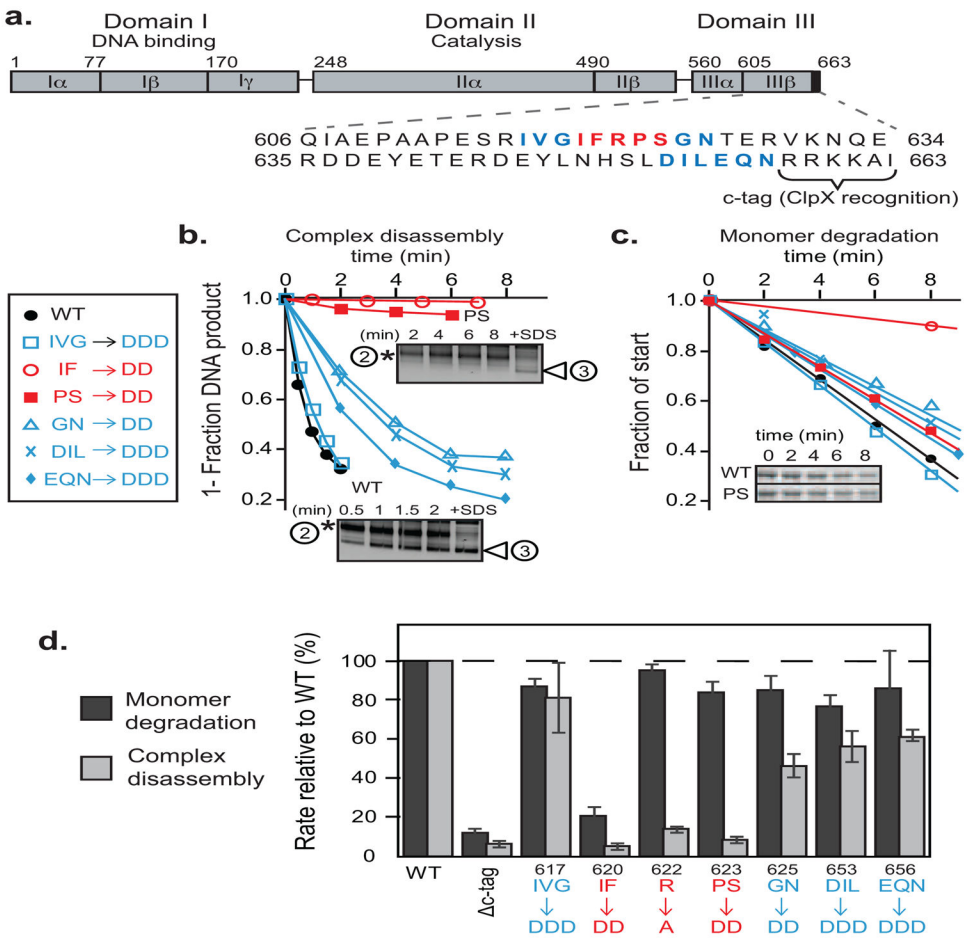

FIGURE 2. A sequence region Ile_{620}-Ser_{624} forms a critical interaction between MuA complexes and ClpX

A) MuA transposase is a ~75kDa protein comprised of three domains. Domain III contains the C-terminal ClpX pore-binding tag, “C-tag”, which is comprised of the last six residues. Sequences that were mutated in this study are in bolded red or blue.

B) ClpX-catalyzed disassembly of complexes that were assembled from wild-type MuA and MuA “aspartate” variants. Initial transpososome concentration was 100nM. Quantification of appearance of the lowermost DNA disassembly product (white arrow) over time. Two representative native agarose gels of wild-type MuA complexes and MuA(P623D, S624D) mutant complexes are shown. The “+SDS” lane shows the pattern of topoisomer migration upon complete disassembly.

C) Degradation of wild-type MuA and MuA “aspartate” variants by ClpXP protease at subsaturating substrate concentrations (1uM). Inset shows a representative SDS-PAGE gel of wild-type MuA and MuA(P623D, S624D) monomers.

D) Quantification of differences in degradation and disassembly rates of MuA variants whose indicated sequences were mutated to alanine or aspartic acid relative to wild-type MuA. Reactions were performed in triplicate. Error bars are the standard error of the mean.

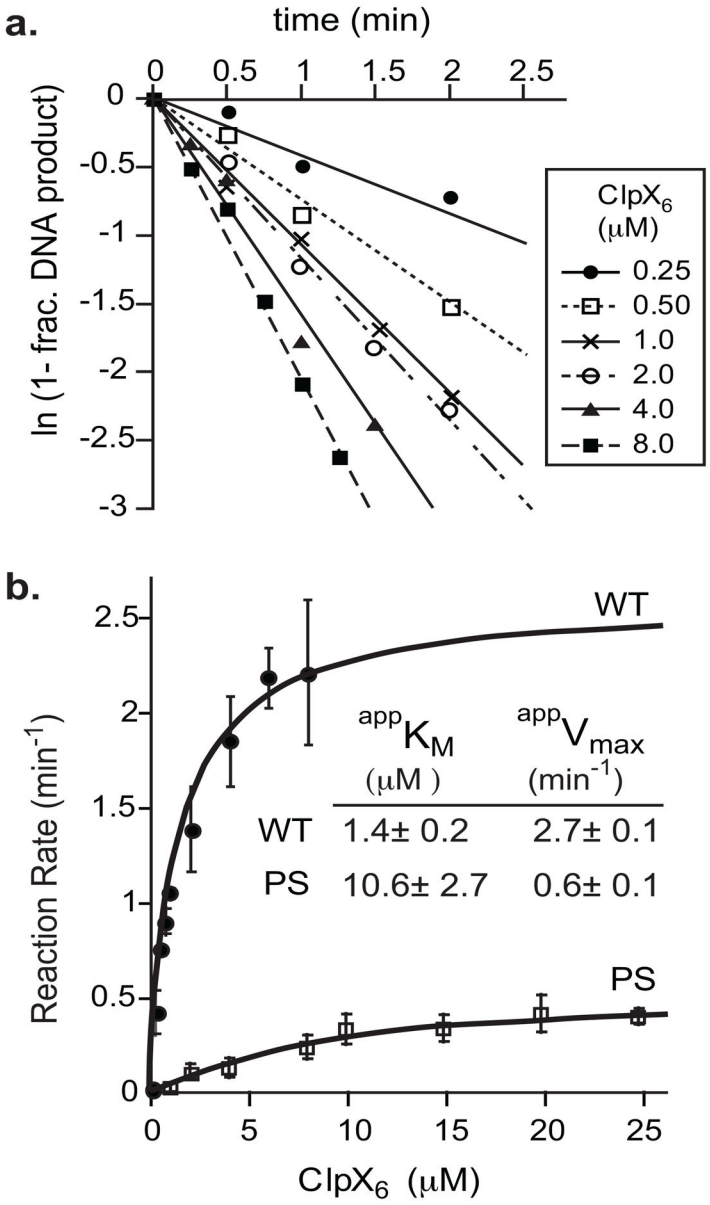

FIGURE 3. Mutation of $P_{623}S_{624}$ leads to a 10-fold reduced apparent affinity between ClpX and transpososomes

A) Disassembly of wild-type MuA complexes by different concentrations of ClpX. Concentration of transpososomes was 100nM.

B) Half-maximal velocity determination for ClpX-mediated disassembly of wild-type complexes and MuA(P623D, S624D) mutant complexes. Curves were repeated in triplicate. Error bars are the standard deviation of the average. Errors of the $^{app}K_M$ are standard deviation of average of three fits.

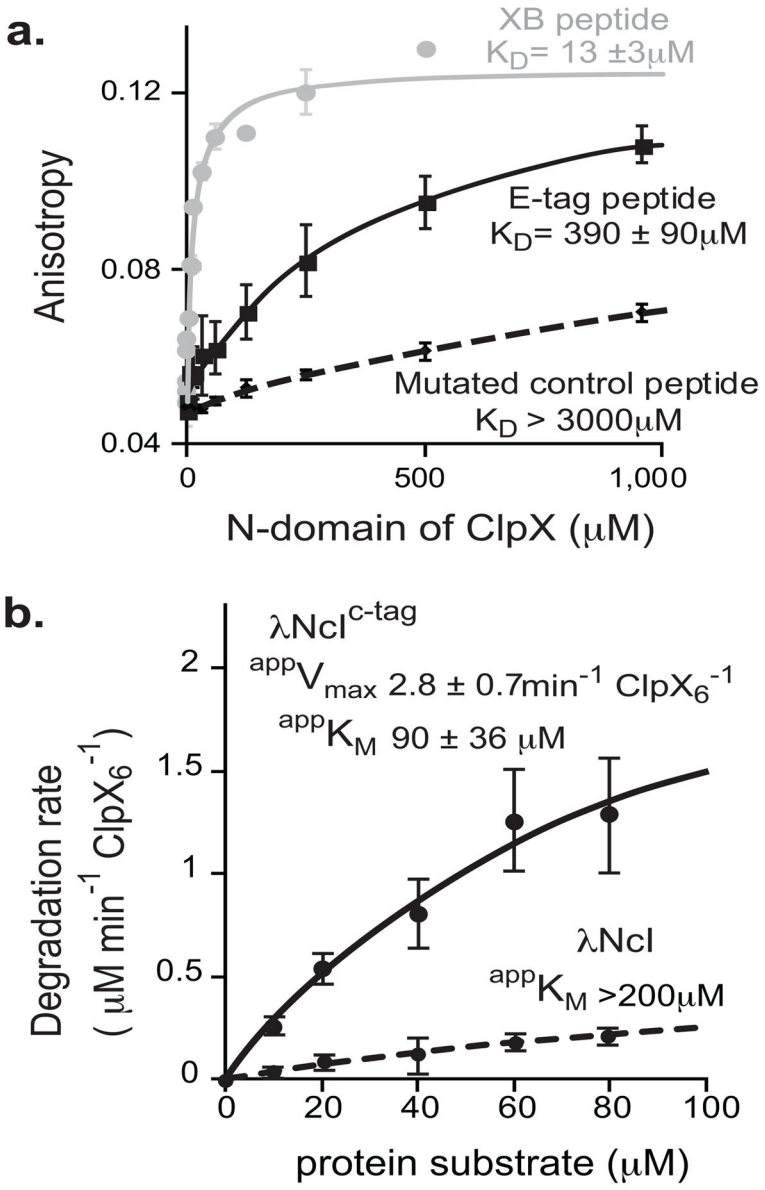

FIGURE 4. Both E-tag and C-tag sequences bind weakly to ClpX

A) Solution binding of N-terminal Fluorescein-labeled peptides and purified N-domain of ClpX. A fixed amount (200nM) of Fluorescein-labeled peptides were incubated with increasing concentrations of purified N-domain. E-tag peptide is ESRIVGIFRPSGNTERVKNQ. A peptide from the ClpX adaptor, SspB, called the XB peptide, which is known to bind the ClpX N-domain was used as a positive control. Its sequence is RGGRPALRVVK. Mutated E-tag control peptide is ESRIVGIFDDDGNTERVKNQ. Errors represent the sample standard deviation where

$$s=\sqrt{\frac{1}{n-1}\sum_{i=1}^{n}(x_i-\overline{x})^2}$$ and $n \geq 2$

B) Half-maximal velocity determination for degradation of $\lambda NcI^{c\text{-}tag}$ by ClpXP. $ClpX_6$ was 0.3μM, $ClpP_{14}$ was 0.8μM, protein substrate as indicated in figure. Negative control was λNcI without the C-tag. Errors represent standard deviation of the average.

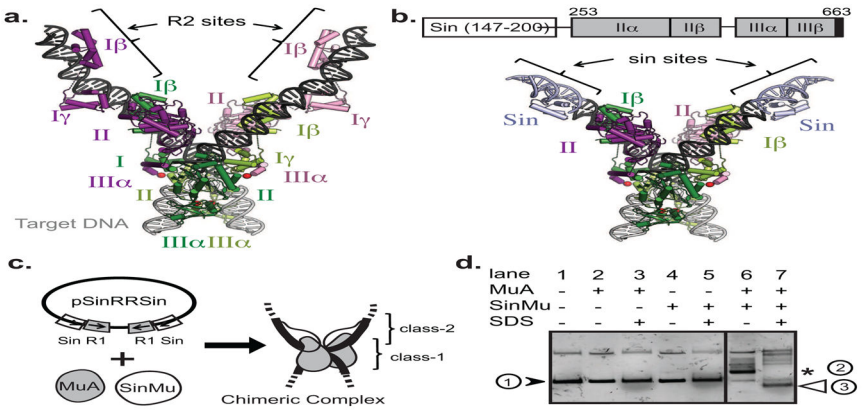

FIGURE 5. Design and construction of SinMu chimeric transpososomes

A) Crystal structure of STC transpososome on two “right-end” oligos (PDB 4FCY) with each subunit in a different color. Subdomains Iβ and Iγ are sequence-specific DNA-binding domains. Pink and purple subunits are bound to R2 sites; green ones to R1 sites. Target DNA is in grey.

B) Model of a chimeric transpososome containing SinMu protein and MuA on DNA fragments carrying the Mu-R1 sites and the Sin-R2 sites. Domain structure of the SinMu chimeric protein, which contains the DNA binding domain of Sin resolvase (147–200; from PDB 2r0q) followed by a linker and MuA domains II and III.

C) The altered- specificity plasmid substrate pSinRRSin has the MuA binding sites, L2 and R2, swapped out for Sin-specific DNA binding sites. This arrangement restricts SinMu protein to the class-2 structural subunits and MuA protein to the class-1 catalytic subunits.

D) Assembly of chimeric complexes on pSinRRSin plasmid requires the presence of both MuA and SinMu proteins. On a native agarose gel, lane 1 contains un-reacted pSinRRSin supercoiled plasmid (black arrow). The *in vitro* assembly reaction shows the band associated with assembled complexes (asterisk) in lane 6, but not in lanes 2 and 4 which each lack one species of protein. The characteristic pattern of recombined DNA disassembly products (white arrow) from a reaction identical to the one in lane 6 is seen after addition of SDS in lane 7.

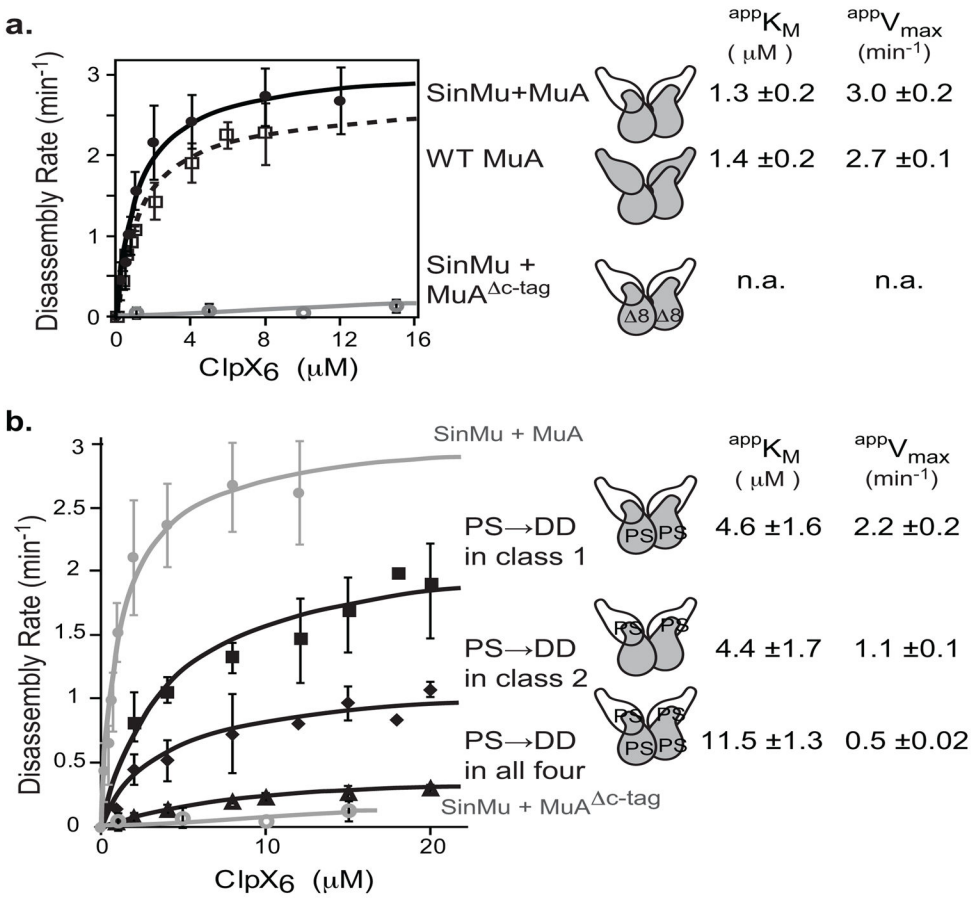

FIGURE 6. Efficient complex disassembly requires E-tags on both class-1 and class-2 subunits

A) Chimeric complex disassembly controls. Half-maximal velocity determination for native and chimeric complexes as indicated. Data for wild-type are superimposed from Figure 3B. Curves were repeated in triplicate. Error bars at each concentration point are the standard deviation of the average. Errors of the $^{app}K_M$ are standard deviation of average of three fits. B) Half-maximal velocity determination for chimeric complexes with different numbers of subunits carrying the mutated E-tag (P623D S624D). SinMu+MuA and SinMu+MuAΔc-tag curves are the same data from (A). Curves were repeated in triplicate. Error bars at each concentration point are the standard deviation of the average. Errors of the $^{app}K_M$ are standard deviation of average of three fits.

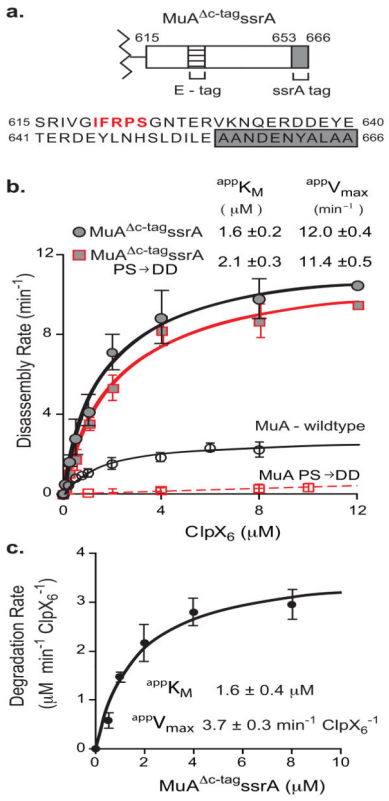

FIGURE 7. ClpX loses discrimination between monomers and transpososomes with a strong Ctag recognition signal

A) Diagram of MuA$^{\Delta c\text{-}tag}$ssrA zoomed in on domain IIIβ and corresponding sequence below. E-tag is in bold red. ssrA tag is in grey box.

B) Half-maximal velocity determination for disassembly of wild-type, MuA (PS/DD), MuA$^{\Delta c\text{-}tag}$ssrA, and MuA$^{\Delta c\text{-}tag}$ssrA (PS/DD) complexes by ClpX. Data for wild-type and MuA (PS/DD) are superimposed from Figure 2D. Reactions were repeated four times. Error bars at each concentration point are standard deviation of the average. Errors of the $^{app}K_M$ are standard deviation of the average of four fits.

C) Half-maximal velocity determination for degradation of MuA$^{\Delta c\text{-}tag}$ssrA monomers by ClpXP. $ClpX_6$ was 0.3μM, $ClpP_{14}$ was 0.8μM. Error bars at each concentration point are standard deviation of the average. Error of the $^{app}K_M$ is standard deviation of the average of three fits.

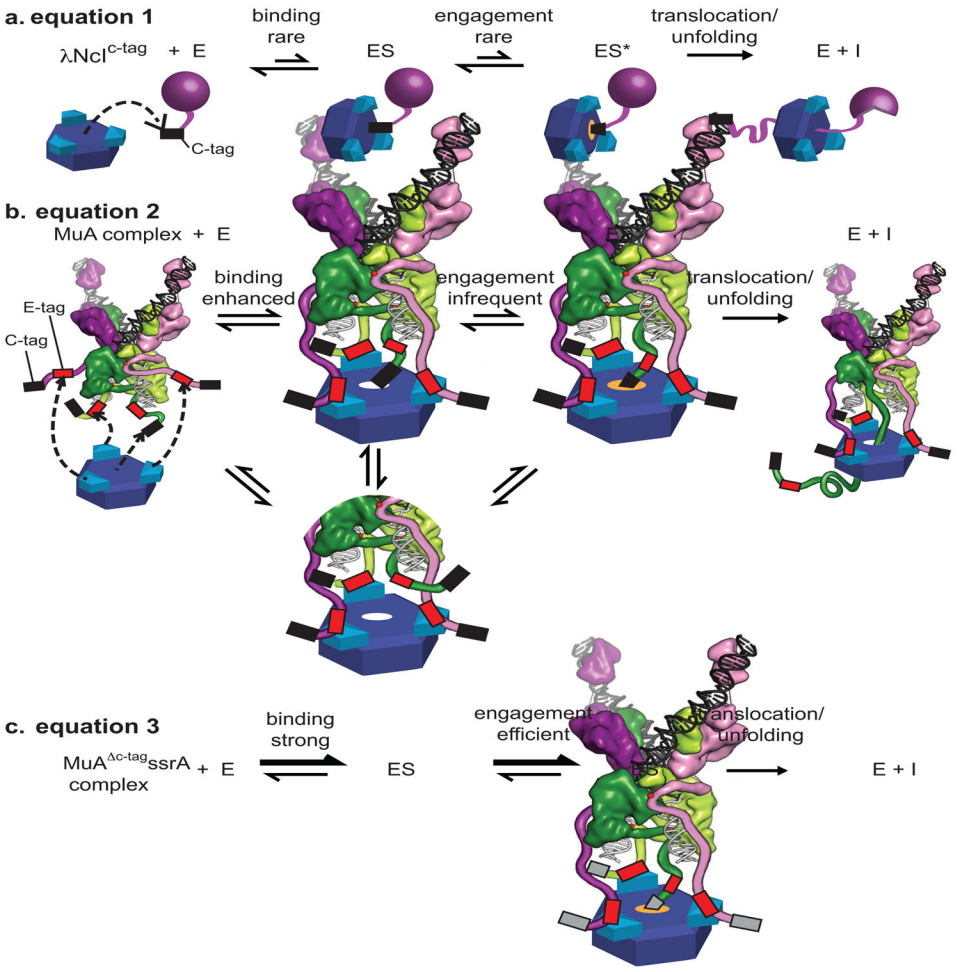

FIGURE 8. Kinetic Model of monomer versus transpososome recognition by ClpX

A) $\lambda NcI^{c\text{-}tag}$ monomer (purple sphere) binds weakly to the pore of ClpX (blue ring) and engagement is rare leading to weak apparent affinities. Engagement of the C-tag (depicted in an orange-glowing pore) leads to a transient enzyme-substrate complex (ES*). After engagement of the Ctag, ClpX processively translocates and unfolds the native protein.

B) Each N-domain dimer (turquoise) in ClpX can bind an E-tag in a wild-type MuA complex (colored as in Fig. 5, with cartooned extensions representing domain IIIβ, red boxes for E-tags and black boxes for C-tags). Binding of a C-tag to the pore of ClpX is enhanced because additional interactions between the E-tags and N-domains of ClpX raise the effective concentration of the C-tag near the pore by restricting the search volume needed for complex formation.

C) In the $MuA^{\Delta c\text{-}tag}$ssrA complex, binding of the ssrA tag to the pore of ClpX is strong. Engagement of the ssrA tag is strong and efficient and occurs similarly whether or not the E-tag is bound to the N-domains of ClpX.

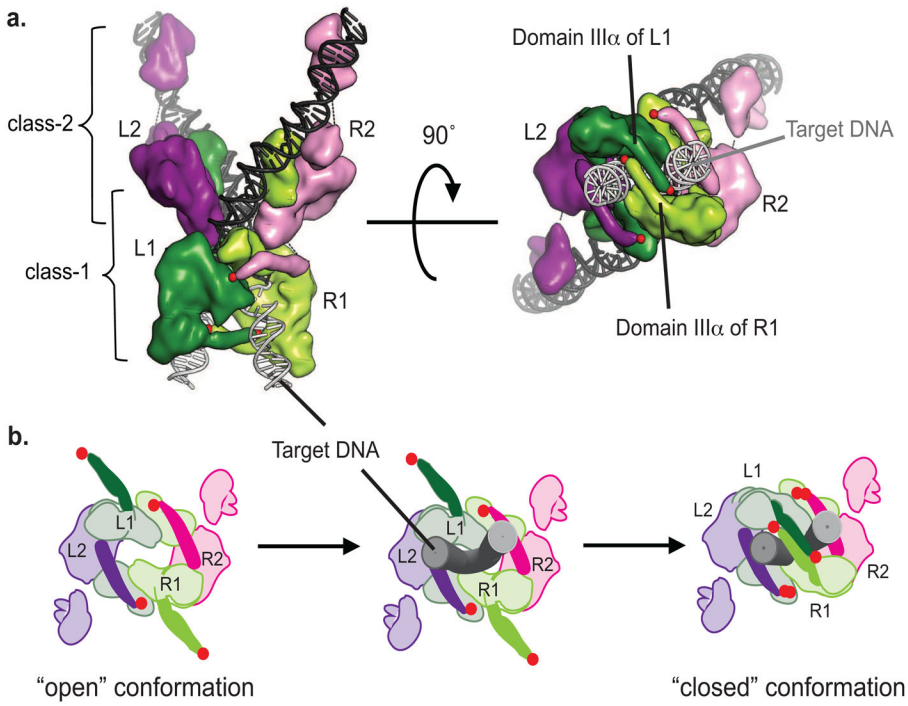

FIGURE 9. Model of conformational changes in MuA complex during transposition

A) Structure-based cartoon of native STC (strand transfer complex); class-1 subunits in dark and light green (L1, R1), class-2 subunits in purple and pink (L2, R2), Mu DNA in black sticks, target DNA in grey sticks. Red dots indicate the C-terminal residue of domain IIIα. Side view on left and "bottom-up" view on right with target DNA coming out from page and Mu DNA facing into the page.

B) Diagram of "bottom-up" view of transpososome indicating proposed conformation changes to allow binding of target DNA. Color scheme same as in (A) with domain IIIα in solid colors and target DNA as gray tubes. After synapsing the left and right ends of the Mu genome, domain IIIa and IIIβ of both class-1 subunits must be in an "open" conformation to allow entry of target DNA brought by MuB. Then these domains swing into a "closed" conformation to trap the target DNA as observed in the crystal structure of the STC.